

## Whole-device linear full-wave simulation of high harmonic ion cyclotron heating in H-mode tokamak plasmas

D. L. Green<sup>1</sup>, E. F. Jaeger<sup>2</sup>, L. A. Berry<sup>1</sup> and P. M. Ryan<sup>1</sup>

<sup>1</sup> Oak Ridge National Laboratory, Oak Ridge, Tennessee 37831-6169, USA

<sup>2</sup> XCEL Engineering Inc., 1066 Commerce Park Dr, Oak Ridge, Tennessee 37830, USA

We present a comparison of NSTX high harmonic fast-wave (HHFW) heating efficiency observations[1, 2] with results from the AORSA[3] whole-device simulation. The simulation retains a realistic geometry and core plasma kinetic physics allowing calculation of the scrape-off plasma linear RF fields. A parametric study of L-mode and neutral beam heated H-mode scenarios quantify the conditions that result in a fast-wave coaxial mode in the scrape-off plasma. These large amplitude coaxial modes are expected to damp on collisions or couple to non-linear damping mechanisms and be correlated to an observed drop in core heating efficiency.

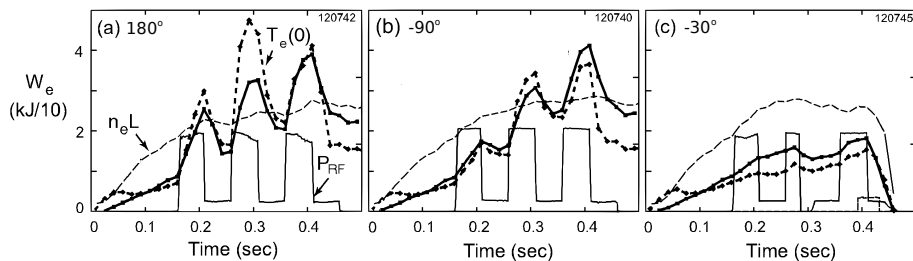


**Figure 1:** Correlation between electron stored energy ( $W_e$ , thick black line) and launched ICRF power ( $P_{RF}$ ) for antenna phasings giving dominant toroidal modes of  $k_\phi = -13 \text{ m}^{-1}$ ,  $-8 \text{ m}^{-1}$  and  $-3 \text{ m}^{-1}$ [1].

Recent observations of improved HHFW heating efficiency on NSTX for both L- (see Fig. 1) and H-mode[2] plasmas show that the fraction of launched ion cyclotron radio frequency (ICRF) power reaching the core plasma is dependent on the antenna strap-to-strap phase difference (the launched toroidal wave-number  $k_\phi$ ), the toroidal magnetic field strength  $B$ , and the scrape-off layer (SOL) density profile in front of the antenna. These observations have been interpreted by Refs. [1, 4] in terms of the location of the fast-wave cutoff whose density is approximately proportional to  $Bk_\phi/\omega$  where  $\omega$  is the angular RF frequency. For NSTX, and most Tokamaks including ITER, this cutoff/onset location sits between the antenna and the separatrix. It is expected that fast-wave propagation in the SOL is correlated with reduced heating efficiency and suggested that excitation of normal modes of the SOL (coaxial modes) between the lossy core plasma and the conducting vacuum structure are the primary cause of the observed degraded HHFW heating efficiency. In this paper we examine full-wave simulation results valid for HHFW on NSTW that include a realistic scrape-off plasma finding that coaxial modes are excited for antenna and edge parameters that correlate with poor heating efficiency shots.

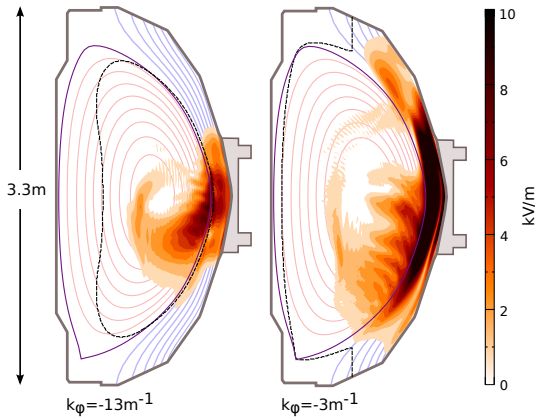


**Figure 2:** H-mode 2-D AORSA electric field amplitude. The dashed line shows an approximate fast-wave cutoff using  $k_{\parallel} \approx k_{\phi} = n_{\phi}/R$ .

The design and simulation of ICRF antenna near field and coupling properties is typically the realm of dedicated antenna codes. Such codes, e.g. TOPICA[5], can handle the actual geometry of the antenna, including the Faraday screen, feeders, etc. Maxwell's equations are solved for vacuum conditions close the antenna coupled to an approximate representation of the core plasma as an inner boundary condition. TOPICA utilizes the FELICE code[6, 7] to numerically calculate impedance and admittance surface matrices giving a hot plasma description under the finite Larmor radius (FLR) approximation. This approach is capable of determining the loading resistance of loop antennas and self-consistently estimates the antenna current distribution  $\vec{J}_a$ . While dedicated antenna codes do resolve the normal modes of the plasma edge of interest in this paper, they approximate the core plasma response and none retain the required kinetic physics to accurately model HHFW. This is typically left to dedicated core plasma codes such as TORIC[8] and AORSA[3]. Here we use an extension to AORSA, which retains all the required kinetic physics to examine HHFW heating on NSTX and resolve normal modes of the SOL. While this version of AORSA does resolve the wave-fields of the SOL, it does not self-consistently calculate the antenna current, nor do we resolve the fine scale features of the antenna and Faraday shield structures.

We present AORSA results for two NSTX scenarios: (i) L-mode helium (shot #120745 at 0.392 s) and (ii) H-mode deuterium with neutral beam injection (NBI) (shot #130608 at 0.353 s). Figure 2 shows the AORSA electric wave-field amplitude for the H-mode scenario. It is clear from Fig. 2 that the magnitude of the wave-fields in the SOL have a dependence on the launched  $k_{\phi}$ . For large  $k_{\phi}$  ( $-13 \text{ m}^{-1}$ ,  $-180^\circ$  antenna phasing) an evanescent wave-field is calculated in the SOL while for small  $k_{\phi}$  ( $-5 \text{ m}^{-1}$ ,  $-30^\circ$  antenna phasing) a large amplitude coaxial standing mode (see the null in the field magnitude) is excited. Figure 3 shows the simulated 3-D electric field amplitude that correlates with reduced efficiency experimental observations for an antenna phasing of  $-30^\circ$  (c.f., Fig. 1(c)). To further characterize under what conditions normal modes of the SOL may be excited, degrading heating efficiency, here we examine the launched  $k_{\phi}$  and scrape-off plasma electron density ( $n_e$ ) parameter space with both a 0-D dispersion analysis and the AORSA full-wave simulation. Figure 4 shows both the zero contour of  $k_{\perp}^2$  (the approximate fast-wave cutoff) as calculated assuming  $k_{\parallel} \approx k_{\phi} = n_{\phi}/R$  and contours of the median SOL

electric wave-field amplitude. Dark areas show excitation of normal modes. These results show an asymmetry in the SOL electric field magnitude with the sign of  $n_\phi$  due to the poloidal field. Also, the coaxial modes are localized to  $\pm n_\phi = 5$  for H- and  $-5 \leq n_\phi \leq 0$  for L-mode. In the L-mode scenario, increasing the density for negative  $n_\phi$  from below the cutoff value (left of the white  $k_\perp^2 = 0$  contour) to above the cutoff shows either excitation of a coaxial mode ( $n_\phi \approx -5$ ) or an increase in the field magnitude ( $n_\phi \approx -20$ ).

The performance of the ITER ion cyclotron heating system has been the subject of several computational studies (e.g., Refs. [9, 10]) showing that the power coupling depends significantly on the antenna-separatrix distance, the density profile of the SOL and the toroidal strap phasing. As such, the conclusions of this work have implications for ITER, where the separatrix-wall distance is large (10 to 20 cm). It may prove difficult to control the edge density in such a large region to below that for fast-wave propagation, especially in the presence of ELMs which may increase the SOL density and increase the RF power deposition to the edge (see Ref. [11]). Assuming an  $n_e$  at the separatrix in

ITER of  $n_0 = 1 \times 10^{19} \text{ m}^{-3}$ , with a decay in the SOL of the form  $n_e(\delta r) = n_0 \exp(-\delta r/l_{\text{SOL}})$  where  $\delta r$  is the distance from the separatrix and  $l_{\text{SOL}} = 4 \text{ cm}$  is the SOL decay length, the onset location for fast-wave propagation for the dominant mode for  $-90^\circ$  antenna phasing ( $n_\phi \approx -32$ ,  $k_\phi = -3.84 \text{ m}^{-1}$ ) is 11 cm from the antenna. This is well within the scrape-off plasma. Therefore, optimizing the SOL density profile will be important for ICRF heating efficiency on ITER.

By means of whole-device full-wave simulation we have shown that ICRF excitation of normal modes of the scrape-off plasma is a probable cause of observed degraded heating efficiency for  $-30^\circ$  antenna phasing on NSTX. As such, increases in the scrape-off plasma density beyond that required for fast-wave propagation (e.g., that caused by ELMs[11]) is likely to degrade ICRF heating efficiency. Also, differences between a simple dispersion analysis calculation of the fast-wave cutoff location and full-wave results showing coaxial mode excitation reveal a need for including an increasing level of realism when predictive capabilities are desired. In particular, this will be an issue for ITER where controlling the edge density to below that for fast-wave propagation may be difficult.

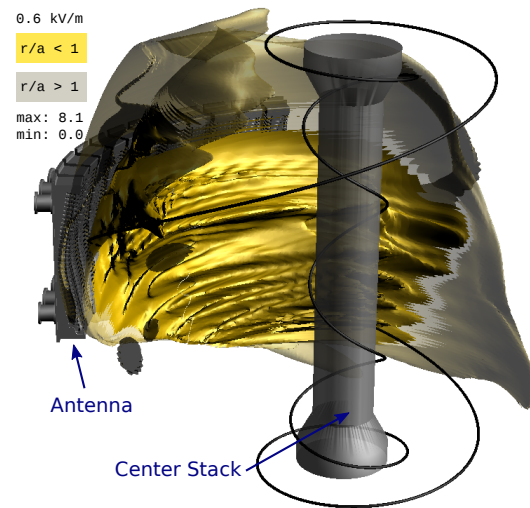


**Figure 3:** H-mode 3-D AORSA electric field amplitude for  $-30^\circ$  antenna phasing. Transparent contours are in the SOL, solid are in the core plasma.

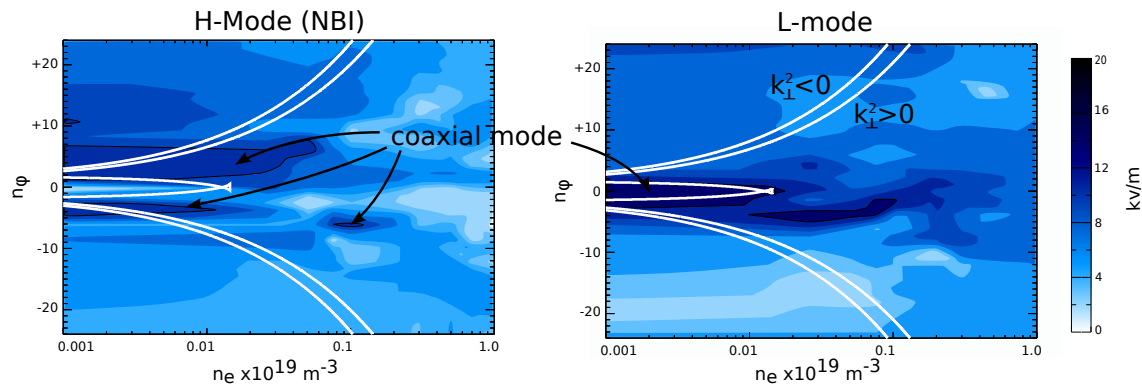


**Figure 4:** Blue contours show the AORSA median SOL RF electric field amplitude. White lines are the zero contour of the  $k_{\perp}^2$  dispersion calculation (i.e., the fast-wave cutoff with propagation and evanescent regions indicated in the right panel) for high-field ( $R = 1.52$  m and  $B_{L\text{-mode}} = 0.34$  T,  $B_{H\text{-mode}} = 0.37$  T), and low-field ( $R = 1.68$  m and  $B_{L\text{-mode}} = 0.33$  T,  $B_{H\text{-mode}} = 0.29$  T) sides of the SOL.

## Acknowledgements

The authors wish to thank Benoit LeBlanc for providing TRANSP NBI profile data. This research used resources of the Oak Ridge Leadership Computing Facility, located in the National Center for Computational Sciences at Oak Ridge National Laboratory, and the National Energy Research Scientific Computing Center supported by the Office of Science of the Department of Energy under Contracts DE-AC05-00OR22725 and DE-AC02-05CH11231 respectively.

## References

- [1] J. Hosea, R. E. Bell, B. P. LeBlanc, C. K. Phillips, G. Taylor, E. Valeo, J. R. Wilson, E. F. Jaeger, P. M. Ryan, J. Wilgen, et al., *Physics of Plasmas* **15**, 056104 (2008).
- [2] G. Taylor, R. E. Bell, J. C. Hosea, B. P. LeBlanc, C. K. Phillips, M. Podesta, E. J. Valeo, J. R. Wilson, J.-W. Ahn, G. Chen, D. L. Green, E. F. Jaeger, et al., *Physics of Plasmas* **17**, 056114 (2010).
- [3] E. F. Jaeger, L. A. Berry, J. R. Myra, D. B. Batchelor, E. D'Azevedo, P. T. Bonoli, C. K. Phillips, D. N. Smithe, D. A. D'Ippolito, et al., *Phys. Rev. Lett.* **90**, 195001 (2003).
- [4] C. Phillips, R. Bell, L. Berry, P. Bonoli, R. Harvey, J. Hosea, E. Jaeger, B. LeBlanc, P. Ryan, G. Taylor, et al., *Nuclear Fusion* **49**, 075015 (2009).
- [5] V. Lancellotti, D. Milanesio, R. Maggiora, G. Vecchi, and V. Kyrytsya, *Nuclear Fusion* **46**, S476 (2006).
- [6] M. Brambilla, *Plasma Physics and Controlled Fusion* **31**, 723 (1989).
- [7] M. Brambilla, *Plasma Physics and Controlled Fusion* **35**, 41 (1993).
- [8] M. Brambilla, *Plasma Physics and Controlled Fusion* **41**, 1 (1999).
- [9] P. Lamalle, A. Messiaen, P. Dumortier, and F. Louche, *Nuclear Fusion* **46**, 432 (2006).
- [10] A. Messiaen, R. Koch, R. Weynants, P. Dumortier, F. Louche, R. Maggiora, and D. Milanesio, *Nuclear Fusion* **50**, 025026 (2010).
- [11] J. C. Hosea, J.-W. Ahn, R. E. Bell, S. Gerhardt, T. K. Gray, D. L. Green, E. F. Jaeger, B. P. LeBlanc, R. Maingi, A. McLean, et al., “The Effect of ELMs on HHFW Heating of NBI Generated H-modes,” in *19th Topical Conference on Radio Frequency Power in Plasmas*, Newport, RI, USA, 2011.